High Proton Conductivity by a Metal Organic Framework Incorporating Zn8O Clusters with Aligned Imidazolium Groups Decorating the Channels

ARTICLE *in* JOURNAL OF THE AMERICAN CHEMICAL SOCIETY · NOVEMBER 2012

Impact Factor: 12.11 · DOI: 10.1021/ja3076378 · Source: PubMed

JACS
JOURNAL OF THE AMERICAN CHEMICAL SOCIETY
Article
pubs.acs.org/JACS

High Proton Conductivity by a Metal–Organic Framework Incorporating Zn_8O Clusters with Aligned Imidazolium Groups Decorating the Channels

Susan Sen,[†] Nisanth N. Nair,[†] Teppei Yamada,[‡] Hiroshi Kitagawa,*[,‡] and Parimal K. Bharadwaj*[,†]

[†]Department of Chemistry, Indian Institute of Technology, Kanpur 208016, India

[‡]Division of Chemistry, Graduate School of Science, Kyoto University, Kitashirakawa-Oiwakecho, Sakyo-ku, Kyoto 606-8502, Japan

Supporting Information

ABSTRACT: A novel metal–organic framework, $[\{(Zn_{0.25})_8(O)\}Zn_6(L)_{12}(H_2O)_{29}(DMF)_{69}(NO_3)_2]_n$ (**1**) {H_2L = 1,3-bis(4-carboxyphenyl)imidazolium}, has been synthesized under solvothermal conditions in good yield. It shows a Zn_8O cluster that is coordinated to six ligands and forms an overall three-dimensional structure with channels along the crystallographic *a* and *b* axes. The imidazolium groups of the ligand moiety are aligned in the channels. The channels are not empty but are occupied by a large number of DMF and water molecules. Upon heating, these solvent molecules can be removed without breakdown of the overall structure of the framework as shown by variable-temperature powder X-ray diffraction patterns. Of great interest is the fact that the compound exhibits high proton conductivity with a low activation energy that is comparable to those of Nafion presently used in fuel cells.

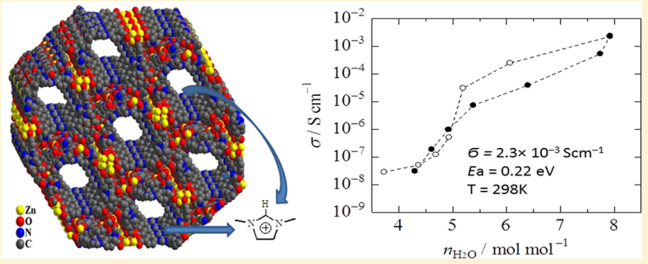

INTRODUCTION

Crystalline metal–organic framework (MOF) structures can be readily and conveniently synthesized in good yields from metal ions and suitable ligands adopting the modular approach and under hydro(solvo)thermal conditions. In robust MOFs, the overall structure remains intact upon removal of solvent molecules occupying the voids leading to porous MOFs. These porous materials are attractive in several contemporary areas of research such as adsorption of gases,[1] chemistry in the coordination space,[2] separation of geometrical isomers,[3] and so on. In recent times, they have attracted increasing attention for potential uses in electrochemical devices and fuel cells as well as probes for studying transport dynamics and biological ion channels.[4] Particularly, porous MOFs are finding more attention as proton-conducting separator materials to replace the existing proton exchange membrane in fuel cells.[5] The polymer Nafion with a perfluorinated backbone and having side chains with sulfonic acid groups as terminals is an important proton-conducting separator material.[6] However, its use is limited to temperatures lower than 80 °C. For fuel cell research, materials that exhibit significant proton conductivity at temperatures above 100 °C are desirable and are highly relevant for clean energy applications. Also, the activation energy should be comparable to that of Nafion (0.22 eV).[7] In this context, porous MOFs, because many of them show thermal stability, offer excellent opportunities as proton-conducting separator materials. In MOFs, designability of the channels in terms of size, shape, and environment allows control over loading of guests into the channels. For enhanced proton conductivity, either organic linkers have been derivatized with sulfonic, phosphonic, carboxylic, or hydroxyl groups[8] that can align themselves in the channels or proton carriers such as imidazole, triazoles, ammonium ions, hydroxonium ions, etc.[9] have been introduced into the empty channels. Increased acidity of metal-bound water molecules inside the channel has also been used as the proton source to a hydroxylic solvent such as methanol.[10] Herein, we provide another interesting system for high proton conductivity. We have used an angular ligand with two aromatic carboxylates at the terminal and an imidazolium group in the middle (Scheme 1a). Aromatic carboxylates have been extensively used[11] as rigid tectons to bind metal centers for the construction of stable coordination polymers. On the other hand, the methylene hydrogens of the imidazolium moiety are highly acidic as deprotonation affords a neutral carbene that can be stabilized due to the presence of two heteroatoms near the carbene center (Scheme 1b).

The potential of the molecular building block (MBB) approach has been recognized for the assembly and development of functional porous MOFs since the discovery of MOF-5 by Yaghi and others.[12] This approach offers fine control over the chemical environment as well as topology of the internal voids using appropriate building blocks. Formation of metal clusters or an inorganic MBB during synthesis of MOFs enhances their robustness and at the same time may increase

Received: August 2, 2012
Published: November 6, 2012

dx.doi.org/10.1021/ja3076378 | J. Am. Chem. Soc. 2012, 134, 19432–19437

Scheme 1. (a) Chemical Structure of the Ligand H_2L^+ and (b) Schematic Representation of the Carbene Generation on Deprotonation of the Methylene Carbon

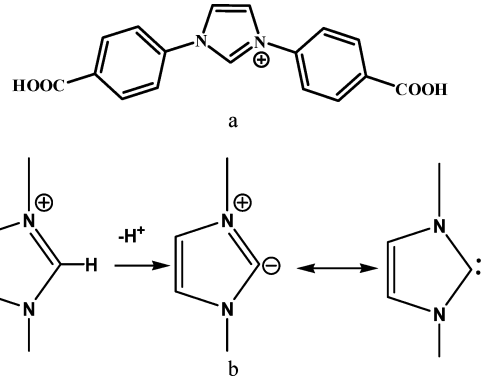

the porosity of the framework. There are several reports on metal clusters of different nuclearities available in the literature.[13] Presently, we describe a porous MOF built with the imidazolium-based ligand (Figure 1a) and a hitherto

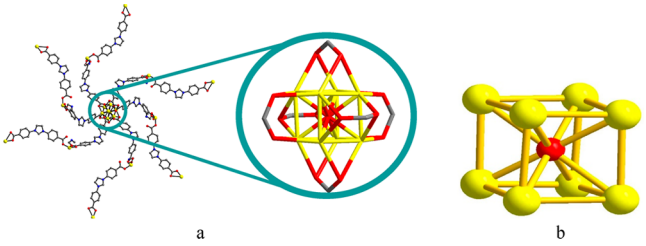

Figure 1. (a) Perspective view of the Zn_8O cluster. (b) Perspective view showing how the Zn_8O cluster is bonded to the carboxylate groups.

unknown $\{Zn_8O\}$ cluster. The overall 3D structure shows channels occupied by a large number of water and DMF molecules that form H-bonded networks. This framework has high thermal stability (~ 400 °C) and shows remarkably high proton conductivity with a low activation energy.

EXPERIMENTAL PROCEDURE

Materials and Method. Reagent grade $Zn(NO_3)_2{\cdot}6H_2O$, 4-aminobenzoic acid, glyoxal (30% aqueous solution), and paraformaldehyde were purchased from Sigma-Aldrich and used without further purification. All solvents were purified following the established procedures prior to use.[14]

Physical Measurements. Spectroscopic data were collected as follows: IR spectra (KBr disk, 400−4000 cm^{-1}) were recorded on a Perkin-Elmer model 1320 spectrometer. Powder X-ray diffraction (PXRD) patterns were recorded with a Bruker D8 Advance diffractometer equipped with nickel-filtered Cu Kα radiation. The tube voltage and current were 40 kV and 40 mA, respectively. Thermogravimetric analysis (TGA) (5 deg/min heating rate under a nitrogen atmosphere) was performed with a Mettler Toledo Star system. ^{1}H NMR spectra were recorded on a JEOL JNM-LA500 FT instrument (500 MHz) in DMSO-d_6 with TMS as the internal standard. Melting points were recorded on an electrical melting point apparatus by PERFIT India and are uncorrected. Elemental analyses were obtained from the Central Drug Research Institute, Lucknow, India.

Synthesis of the ligand 1,3-bis(4-carboxyphenyl)imidazolium chloride ($H_2L^+Cl^-$) was achieved in several steps following a literature procedure[15] after slight modification.

Synthesis of *N,N′*-Bis(4-carboxyphenyl)ethylenediimine (L_1). 4-Aminobenzoic acid (10 g, 2.0 equiv) was dissolved in dry methanol (30 mL). Formic acid (4 drops) was added followed by dropwise addition of a 30% aqueous solution of glyoxal (5.3 mL, 1.0 equiv). The solution was stirred at ambient temperature for 24 h. The white solid formed was collected by filtration, washed with cold methanol, and dried in air. Yield: 65%. Mp: >300 °C. ^{1}H NMR (500 MHz, DMSO-d_6, 25 °C, TMS, δ): 7.72 (d, 2H, Ar*H*), 7.91 (d, 2H, Ar*H*), 8.23 (d, 2H, Im*H*). ESI-MS (m/z): 296 (100) $[L_1]^+$. Anal. Calcd for $C_{16}H_{12}N_2O_4$: C, 64.86; H, 4.08; N, 9.45. Found: C, 64.96; H, 4.01; N, 9.55.

Synthesis of 1,3-Bis(4-carboxyphenyl)imidazolium Chloride ($H_2L^+Cl^-$). Compound L_1 (5 g, 16.89 mmol), as obtained above, was dissolved in anhydrous THF (10 mL) under an argon atmosphere followed by addition of a solution of paraformaldehyde (635 mg, 21.16 mmol,1.25 equiv) in 12 N HCl (2.1 mL, 25.33 mmol, 1.5 equiv) in dioxane (4 mL) at 0 °C. The reaction mixture was stirred at room temperature for 4 h. The light pink precipitate formed was collected by filtration, washed with Et_2O, and dried in vacuum. Yield: 70%. Mp: >300 °C. ^{1}H NMR (500 MHz, DMSO-d_6, 25 °C, TMS, δ): 7.97 (d, 2H, Ar*H*), 8.16 (d, 2H, Ar*H*), 8.48 (d, 2H, Im*H*), 10.40 (s, 1H, Im*H*). ESI-MS (m/z): 309 (100) $[H_2L]^+$. Anal. Calcd for $C_{17}H_{13}N_2O_4Cl$: C, 59.22; H, 3.80; N, 8.12. Found: C, 60.05; H, 3.72; N, 8.21.

Synthesis of $[\{(Zn_{0.25})_8(O)\}Zn_6(L)_{12}(H_2O)_{29}(DMF)_{69}(NO_3)_2]_n$ (1). This compound was synthesized by mixing 1 mmol of $H_2L^+Cl^-$ and 4 mmol of $Zn(NO_3)_2{\cdot}6H_2O$ in 3 mL of DMF in a Teflon-lined autoclave. It was heated under autogenous pressure to 120 °C for 48 h. Cooling to room temperature at the rate of 10 °C/h afforded the product as colorless thin crystals in ~40% yield. Anal. Calcd for $C_{411}H_{697}N_{95}O_{152}Zn_8$: C, 49.74; H, 7.08; N, 13.40. Found: C, 50.17; H, 6.89; N, 13.54.

X-ray Structural Studies. Single-crystal X-ray data were collected at 100 K on a Bruker SMART APEX CCD diffractometer using graphite-monochromated Mo Kα radiation (λ = 0.71069 Å). The linear absorption coefficients, scattering factors for the atoms, and anomalous dispersion corrections were taken from the International Tables for X-ray Crystallography. Data integration and reduction were processed with SAINT[16a] software. An empirical absorption correction was applied to the collected reflections with SADABS[16b] using XPREP.[16c] The structure was solved by the direct method using SHELXTL[16d] and was refined on F^2 by the full-matrix least-squares technique using the SHELXL-97[16e] program package. The unit cell includes a large region of disordered solvent molecules, which could not be modeled as discrete atomic sites. We employed PLATON/SQUEEZE to calculate the diffraction contribution of solvent molecules and thereby to produce a set of solvent-free diffraction intensities. The structure was then refined again using the data generated. The lattice parameters and structural data are collected in Table S1 (Supporting Information). Crystallographic data for the structure reported in this paper have also been deposited with the CCDC as deposition no. CCDC 875410 (available free of charge, on application to the CCDC, 12 Union Rd., Cambridge CB2 1EZ, U.K.; e-mail deposit@ccdc.cam.ac.uk).

Water Uptake Measurements. Water adsorption isotherms of compound **1** were collected volumetrically using a BELSORP-max apparatus (BEL Japan). Measurements were executed after elimination of guests by evacuation of the sample at 80 °C for over 4 h.

Ac Impedance Measurements. Proton conductivity was measured using the conventional quasi four-probe method. The diameter of the pellet was ca. 5 mm ⌀, which was estimated by the jigs. The thickness of the pellet was 0.81 mm, measured by a thickness gauge (Absolute 547-301, Mitutoyo Co. Ltd., Japan, accuracy 0.01 mm). The specimen was compacted, and gold wires were attached to both sides of the pellet with gold paste. Ac impedance measurements were carried out with 4294A (Agilent) and 1260 (Solartron) impedance analyzers under controlled temperature and humidity conditions by an incubator (SH-221, ESPEC Co. Ltd., Japan). Each conductivity measurement was executed more than 12 h after the humidity condition was set. The measurement was repeated several times to confirm that the conductivity became stabilized. The

dx.doi.org/10.1021/ja3076378 | J. Am. Chem. Soc. 2012, 134, 19432−19437

contributions for the resistance by the proton conductivity were estimated using the Nyquist plots.

Theoretical Calculations. To scrutinize the bonding of the $[Zn_8O(CO_2)_6]^{8+}$ cluster, we have performed electronic structural analysis based on density functional theory in its plane wave pseudopotential formulation, as implemented in the Quantum ESPRESSO[17a] package. All calculations were carried out using the gas-phase model $[Zn_8O(HCO_2)_6]^{8+}$, with the positions of H atoms energy minimized and keeping the heavy -atoms fixed at their X-ray crystallographic positions. A finite boundary condition with a cubic box of 14 Å was taken. The PBE[17b] exchange-correlation functional was chosen, and the core electrons were taken into account using the ultrasoft pseudopotentials[17c] with a plane-wave cutoff of 30 Ry. Both 3d and 4s valence electrons of Zn were explicitly included in the calculations. Löwdin charges of atoms were computed using the projection of the Kohn–Sham orbitals on the orthogonal pseudo atomic orbitals.

RESULTS AND DISCUSSION

Compound **1** was synthesized solvothermally at 120 °C by reacting the ligand with $Zn(NO_3)_2{,}6H_2O$ in a 1:4 molar ratio. Satisfactory elemental analysis was achieved for the formulation, and all major peaks of experimental and simulated PXRD from the single-crystal structure are well matched, confirming the phase purity. Once isolated, it is highly stable in air and insoluble in water and in common organic solvents such as acetone, methanol, ethanol, chloroform, DMF, and DMSO. Thermal analysis of **1** shows that weight loss takes place in three steps. The first weight loss occurs in the temperature range of 50–80 °C (11.2%), the second weight loss of 17.3% takes place between 140 and 160 °C, and the final weight loss of 27.1% occurs between 270 and 300 °C. The total weight loss of 55.6% below 320 °C corresponds to the liberation of 69 DMF and 29 water molecules per formula unit. Complete decomposition of the compound is achieved beyond 400 °C (Figure S1, Supporting Information).

The compound crystallizes in the trigonal space group $R\bar{3}$. The structure can be described as six different ligand units bonded to a metal cluster via bridging carboxylates. The other end of each ligand is bonded to a single tetrahedral Zn(II) ion (Figure 1a). An interesting feature of this structure is the presence of a hitherto unknown metal cluster where eight hepta-coordinated Zn(II) ions occupy the corners of a cuboid with an O^{2-} ion at the body center (Figure 1b). While the lone O atom lies on a 6-fold symmetry axis, one of the Zn^{2+} ions lies on a 3-fold symmetry axis so that crystallographic requirements lead to the Zn_8O cluster. The dimensions of the approximate cuboid are 2.247(2) × 2.247(2) × 2.183(4) $Å^3$. Another plausible explanation can be a Zn_4O cluster with Zn ions disordered over two positions. Earlier reports[18] mention the presence of a $\{Zn_4O\}$ cluster due to positional disorder of the Zn^{2+} ions.

The extended structure contains another subunit of a 48-membered metallomacrocycle constructed from three ligands and three tetrahedral Zn(II) ions. Coordination of each tetrahedral Zn(II) ion consists of one chelated and one bridging carboxylate with the fourth coordination site occupied by a DMF molecule. The approximate diameter of the metallomacrocycle is 17.6 Å. Six such metallomacrocycles are connected through a ligand unit to the metal cluster (Figure 2), resulting in an extended 2D sheet structure.

These 2D sheets interpenetrate into each other and are locked by a chain-lock mechanism, i.e., 6,3-connected 3-fold interpenetration (Figure S5, Supporting Information), propagating in all dimensions. The overall structure shows channels along the crystallographic *a* and *b* axes. An interesting feature of this structure is that the methylene groups of the imidazolium moieties are aligned inside the channels (Figure 3) such that they are exposed to any solvent molecule entering the channels.

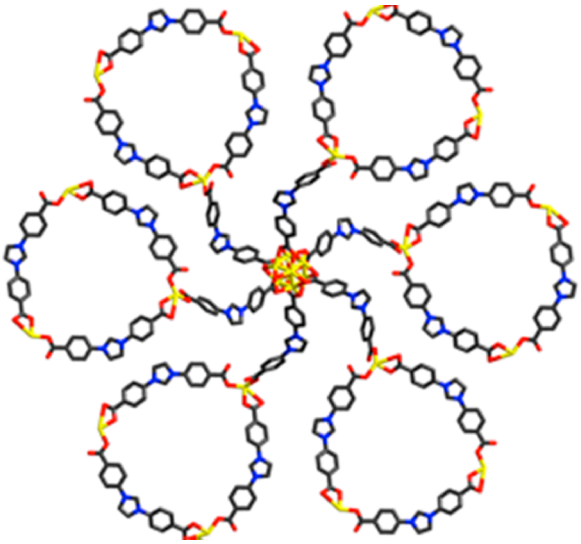

Figure 2. Six metallomacrocycles connected to the core $\{Zn_8O\}$ cluster.

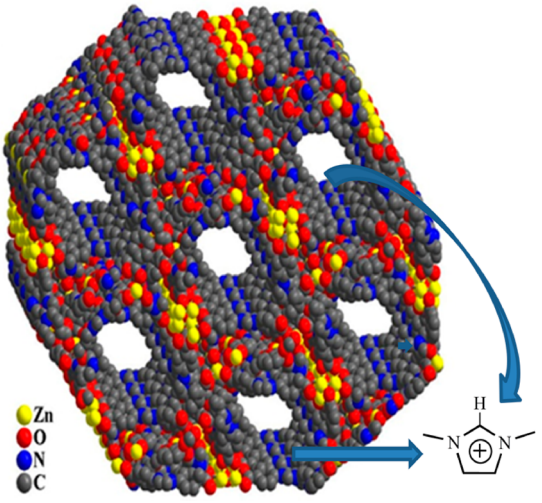

Figure 3. Space-filling diagram along the *a* axis showing methylene groups of the imidazolium moieties are aligned inside the channels.

The channels are not empty but contain solvent molecules, viz., water and DMF along with nitrate anions to balance the charge. The broad peak at 3423 cm^{-1} in the IR spectrum of the complex indicates the presence of water molecules in the structure. Sharp peaks at 1659 and 1625 cm^{-1} appear for free and coordinated CO stretching vibrations of dimethylformamide molecules, respectively, inside the channels. Another sharp peak at 1384 cm^{-1} appears due to the presence of the nitrate anions (Figure S7, Supporting Information). The solvent guest molecules can be removed by heating without structure breakdown. The framework is quite stable, confirmed by the variable-temperature PXRD study (Figure S8, Supporting Information) in the temperature range of 0–250 °C.

dx.doi.org/10.1021/ja3076378 | J. Am. Chem. Soc. 2012, 134, 19432–19437

To obtain a detailed understanding of bonding within the $\{Zn_8O\}$ cluster, we have looked at the atomic orbital contributions to the molecular orbitals of the cluster using the projected density of states (PDOS) of the gas-phase $[Zn_8O(HCO_2)_6]^{8+}$cluster. In Figure 4a, the total PDOS of the

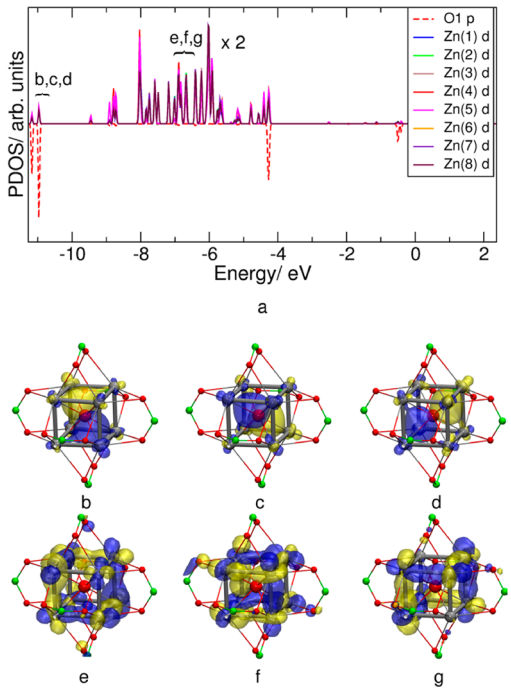

Figure 4. (a) PDOS of the $[Zn_8O(HCO_2)_6]^{8+}$ cluster in vacuo and (b–g) selected molecular orbitals. O1 is the oxygen atom at the center of the Zn_8O cluster. The Fermi energy is set to 0 eV. For clarity in presentation, the total PDOS curve of the O1 p orbitals is drawn along the negative *y* axis. The positions of the orbitals in (b)–(g) are indicated in (a). Atom color code: Zn (black), O (red), C (green), H (gray). Wave functions are visualized as isosurfaces with an isovalue of ±0.0015 (yellow/blue).

p-orbitals of the oxygen, O1, at the center of the $\{Zn_8O\}$ cluster is plotted together with those of the d-orbitals of all eight Zn atoms. Clearly, the O1 p-orbitals overlap with the d-orbitals of the Zn atoms as shown in Figure 4b–d. These three nearly degenerate orbitals are composed of p-orbitals of O1 and d-orbitals of all the Zn atoms. Most importantly, we have observed the existence of Zn–Zn bonds. A few of the orbitals that are involved in the Zn–Zn bonding are presented in Figure 4e–g. It is clear from these figures that Zn–Zn bonds have large contributions from the d-orbitals. In fact, all these orbitals are multicentered, although a single molecular orbital alone encompassing all eight Zn atoms is not observed. Zn atoms are bonded to their nearest neighbors along the sides of the cube, as evident from the molecular orbitals (Figure 4e–g). Calculated Löwdin charges on Zn and O1 of +1.45 and −1.35 e, respectively, confirm the formal oxidation states of +2 for Zn and −2 for O1.

Proton conductivity was evaluated by ac impedance spectroscopy using a compacted pellet of the powdered sample with two gold electrodes attached to the surface. As shown in Figure 5, proton conductivity of **1** increases with an increase of humidity and reaches 2.3×10^{-3} S cm^{-1} at ambient temperature and 95% relative humidity (RH). Slight hysteresis can be observed between adsorption and desorption of water

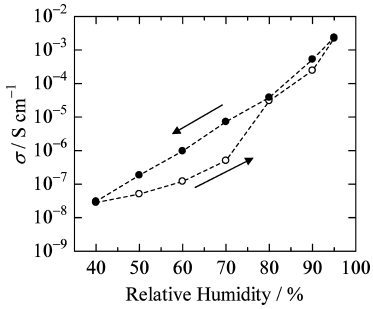

Figure 5. Proton conductivity dependence on humidity at 298 K. The measurement was executed with an increase (open circles) and a decrease (closed circles) in humidity.

(Figure 5). As shown in Figure 6, a hysteresis can also be observed between the water adsorption and desorption

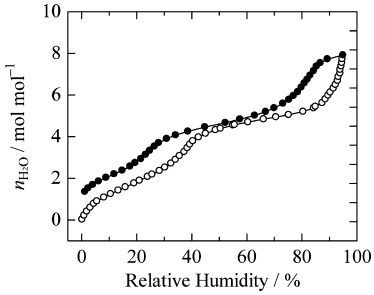

Figure 6. Water adsorption (open circles) and desorption (filled circles) isotherms of **1** at 298 K.

isotherms of **1**, and the proton conductivity depends on the water amount inside the pore of the MOF. The PCT curve has three plateau regions at two, five, and eight water molecules per formula as shown in Figure 7, and the compound has three

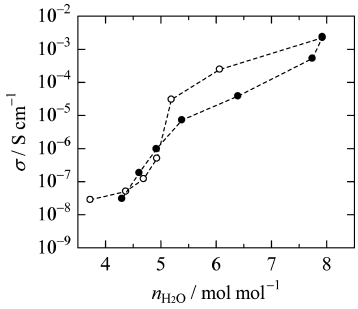

Figure 7. Proton conductivity dependence on water uptake. Conductivity was measured with an increase (filled circles) and a decrease (open circles) of the water content.

hydrated states. We plotted proton conductivity as a function of the water content as shown in Figure 7. The proton conductivity of **1** up to the tetrahydrate state is low. However, addition of the fifth water molecule enhances its conductivity significantly, suggesting that the water molecules in the channel play an important role in the proton conduction. It can be seen from Figure 5 that five water molecules are gradually adsorbed from 40% to 70% RH, and the hysteresis observed in Figure 5 at the humidity range mentioned above is due to the slight hysteresis observed in the adsorption isotherm shown in Figure 6. Large hysteresis can be observed from 80% to 95% RH in the PCT curve (Figure 6). From the plot of proton conductivity

dx.doi.org/10.1021/ja3076378 | J. Am. Chem. Soc. 2012, 134, 19432–19437

dependence on the water uptake (Figure 7), it is found that change in the conductivity above five water molecules is limited and the hysteresis observed is also less prominent (Figure 5).

Temperature dependency of the conductivity was measured, and an Arrhenius plot was obtained as shown in Figure 8. The

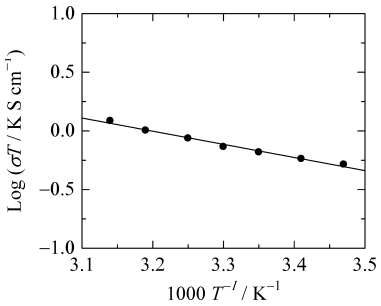

Figure 8. Arrhenius plot of the proton conductivity at 95% RH.

activation energy (E_a) was estimated to be 0.22 eV by applying eq 1. This value is comparable to that of Nafion and lower than

$$\sigma T = \sigma_0 \exp(Ea/kT) \quad (1)$$

those of most MOF systems reported. According to our best knowledge, the lowest reported activation energy for such an MOF system is 0.137 eV for In-5TIA reported by Banerjee et al.[19] and the maximum reported value is 0.63 eV reported by Kitagawa et al.[9c] According to the literature,[4h] we believe that water molecules in the cavity provide the conducting pathway for Grotthuss-type conduction of protons and a high conductivity value is indicative of a high carrier concentration originating from acidic methylene protons lined along each channel. Further analysis is required for determining its conduction mechanism.

In conclusion, we have presented here an unprecedented $\{Zn_8O\}$ cluster that acts as a new type of SBU. This framework leads to a highly porous structure where the pores are occupied by DMF and water molecules. Methylene protons of the imidazolium groups are aligned inside the channel along the crystallographic *a* and *b* axes. This compound shows low conductivity up to the tetrahydrate stage, but once the fifth water molecule is introduced, it shows high proton conductivity with a low activation energy, both of which are comparable to those of Nafion. The water molecules in the channels take part in the Grotthuss-type conduction of protons originating from the methylene protons of the imidazolium groups. Presently, modification of the ligand moiety to alter proton conductivity is being probed.

■ ASSOCIATED CONTENT

Ⓢ Supporting Information

Spectroscopic, thermogravimetric, and powder X-ray diffractometer analyses of compound **1**, crystallographic table including X-ray crystallographic data and a structure for compound **1**, complete ref 17, and CIF data. This material is available free of charge via the Internet at http://pubs.acs.org.

■ AUTHOR INFORMATION

Corresponding Author

pkb@iitk.ac.in; kitagawa@kuchem.kyoto-u.ac.jp

Notes

The authors declare no competing financial interest.

■ ACKNOWLEDGMENTS

We gratefully acknowledge financial support from the Department of Science and Technology, New Delhi, India (to P.K.B.), and SRFs from the Council of Scientific and Industrial Research, New Delhi, India (to S.S.). We thank Prof. R. J. Butcher for his help during structure solution.

■ REFERENCES

(1) (a) Yan, Y.; Telepene, I.; Yang, S.; Lin, X.; Kockelmann, W.; Dailly, A.; Blake, A. J.; Lewis, W.; Walker, S. G.; Allan, D. R.; Barnett, S. A.; Champness, N. R.; Schroder, M. *J. Am. Chem. Soc.* **2010**, *132*, 4092−4094. (b) Kaye, S. S.; Dailly, A.; Yaghi, O. M.; Long, J. R. *J. Am. Chem. Soc.* **2007**, *129*, 14176−14177. (c) Zhao, X.; Xiao, B.; Fletcher, A. J.; Thomas, K. M.; Bradshaw, D.; Rosseinsky, M. J. *Science* **2004**, *306*, 1012−1015. (d) Murray, L. J.; Dinca, M.; Long, J. R. *Chem. Soc. Rev.* **2009**, *38*, 1294−1314. (e) Seki, K.; Mori, W. *J. Phys. Chem. B* **2002**, *106*, 1380−1385. (f) Takamizawa, S.; Nakata, E.-I.; Yokoyama, H.; Mochizuki, K.; Mori, W. *Angew. Chem., Int. Ed.* **2003**, *42*, 4331−4334.

(2) (a) Ma, L.; Abney, C.; Lin, W. *Chem. Soc. Rev.* **2009**, *38*, 1248−1256. (b) Lee, J.; Farha, O. K.; Roberts, J.; Scheidt, K. A.; Nguyen, S. T.; Hupp, J. T. *Chem. Soc. Rev.* **2009**, *38*, 1450−1459.

(3) (a) Li, J.-R.; Kuppler, R. J.; Zhou, H.-C. *Chem. Soc. Rev.* **2009**, *38*, 1477−1504. (b) Britt, D.; Furukawa, H.; Nang, B.; Glover, T. G.; Yaghi, O. M. *Proc. Natl. Acad. Sci. U.S.A.* **2009**, *106* (49), 20637−20640. (c) Bastin, L.; Barcia, P. S.; Hurtado, E. J.; Silva, J. A. C.; Rodrigues, F. E.; Chen, B. *J. Phys. Chem. C* **2008**, *112*, 1575−1581. (d) Das, M. C.; Bharadwaj, P. K. *J. Am. Chem. Soc.* **2009**, *131*, 10492−10949.

(4) (a) Wood, B. C.; Marzari, N. *Phys. Rev. B* **2007**, *76*, 134301−134314. (b) Kreuer, K. D.; Paddison, S. J.; Spohr, E.; Schuster, M. *Chem. Rev.* **2004**, *104*, 4637−4678. (c) Hickner, M. A.; Ghassemi, H.; Kim, Y. S.; Einsla, B. R.; McGrath, J. E. *Chem. Rev.* **2004**, *104*, 4587−4612. (d) Akutu-Sato, A.; Akutsu, H.; Turner, S. S.; Day, P.; Probert, M. R.; Howard, J. A. K.; Akutagawa, T.; Takeda, S.; Nakamura, T.; Mori, T. *Angew. Chem., Int. Ed.* **2005**, *44*, 292−295. (e) Steele, B. C.; Heinzel, A. *Nature* **2001**, *414*, 345−352. (f) Saiz, L.; M. Klein, L. *Acc. Chem. Res.* **2002**, *35*, 482−489. (g) Sapronova, A.; Bystrov, V. S.; Green, M. E. *Front. Biosci.* **2003**, *8*, 1356−1370. (h) Colomban, P. Proton Conductors: Solids, Membranes and Gels—Materials and Devices. *Chemistry of Solid State Materials*; Cambridge University Press: Cambridge, U.K., 1992; Vol. 2. (i) Zhou, Z.; Li, S.; Zhang, Y.; Liu, M. *J. Am. Chem. Soc.* **2005**, *127*, 10824−10825.

(5) (a) Kitagawa, H. *Nat. Chem.* **2009**, *1*, 689−690. (b) Yamada, T.; Sadakiyo, M.; Kitagawa, H. *J. Am. Chem. Soc.* **2009**, *131*, 3144−3145.

(6) Maruitz, K. A.; Moore, R. B *Chem. Rev.* **2000**, *104*, 4535−4585.

(7) Hainovsky, N. G.; Pavlukhin, Y. T.; Hairetdinov, E. F. *Solid State Ionics* **1986**, *20*, 249−253.

(8) (a) Yamada, T.; Morikawa, S.; Kitagawa, H. *Bull. Chem. Soc. Jpn.* **2010**, *83*, 42−48. (b) Shigematsu, A.; Yamada, T.; Kitagawa, H. *J. Am. Chem. Soc.* **2011**, *133*, 2034−2036. (c) Taylor, J. M.; Mah, R. K.; Moudrakouvski., I L; Shimizu, G. K. H. *J. Am. Chem. Soc.* **2010**, *132*, 14055−14057. (d) Umeyama, D.; Horike, S.; Inukai, M.; Itakawa, T.; Kiatagawa, S. *J. Am. Chem. Soc.* **2012**, *134*, 12780−12785.

(9) (a) Brueekaew, S.; Horike, S.; Higuchi, M.; Mizuno, M.; Kawamura, T.; Tanaka, D.; Yanai, N.; Kitagawa, S *Nat. Mater.* **2009**, *8*, 831−836. (b) Hurd, J. A.; Vaidyanathan, R.; Thangadurai, V.; Ractcliffe, C.; Moudrakovski, I. L.; Shimizu, G. K. H. *Nat. Chem.* **2009**, *1*, 705−710. (c) Sadakiyo, M.; Yamada, T.; Kitagawa, H. *J. Am. Chem. Soc.* **2009**, *131*, 9906−9907. (d) Kobayashi, Y.; Jacobs, B.; Allendorf, M. D.; Long, J. R. *Chem. Mater.* **2010**, *22*, 4120−4122.

(10) Jeong, N. C.; Samanta, B.; Lee, C. Y.; FArha, O. K.; Hupp, J. T. *J. Am. Chem. Soc.* **2009**, *134*, 51−54.

(11) (a) Rao, C. N. R.; Natarajan, S.; Vidhyanathan, R. *Angew. Chem., Int. Ed.* **2004**, *43*, 1466−1496. (b) Coronado, E.; Galan-Mascaros, J.

R.; Gomez-Garcia, C. J.; Laukhin, V. *Nature* **2000**, *408*, 447−449. (c) Zheng, Y.-Z.; Xue, W.; Zhang, W.-X.; Tong, M.-L.; Chen, X.-M.; Grandjean, F.; Long, G. J.; Ng, S.-W.; Panissod, P.; Drillon, M. *Inorg. Chem.* **2009**, *48*, 2028−2042.
(12) (a) Li, H.; Eddaudi, M.; O'Keeffe, M.; Yaghi, O. M. *Nature* **1999**, *402*, 276−279. (b) Mori, W.; Inoue, F.; Yoshida, K.; Nakayama, H.; Takamizawa, S.; Kishita, M. *Chem. Lett.* **1997**, 1219−1220.
(13) (a) Tranchemontagne, D. J.; Mendoza-Cortés, J. L.; O'Keeffe, M.; Yaghi, O. M. *Chem. Soc. Rev.* **2009**, *38*, 1257−1283. (b) Moulton, B.; Lu, J.; Hajndl, R.; Hariharan, S.; Zarowthko, M. J. A. *Angew. Chem., Int. Ed.* **2002**, *114*, 2821−2824. (c) Eddaoudi, M.; Kim, J.; Vodak, D.; Sudik, A.; Watchter, J.; O'Keeffe, M.; Yaghi, O. M. *Proc. Natl. Acad. Sci. U.S.A.* **2002**, *99*, 4900−4904. (d) Yaghi, O. M.; Davis, C. E.; Li, G.; Li, H. *J. Am. Chem. Soc.* **1997**, *119*, 2861−2868.
(14) (a) Perrin, D. D.; Armarego, W. L. F. *Purification of Laboratory Chemicals*; Pergamon Press: New York, 1980; see also references therein. (b) Furniss, B. S., Hannaford, A. J.; Smith, P. W. G.; Tatchel, A. R. *Vogel's Textbook of Practical Organic Chemistry*, 5th ed.; Pearson: Harlow, U.K., 1989; see also references therein.
(15) Suessner, M.; Plenio, H. *Chem. Commun.* **2005**, *43*, 5417−5419.
(16) (a) *SAINT+*, version 6.02; Bruker AXS: Madison, WI, 1999. (b) Sheldrick, G. M. *SADABS, Empirical Absorption Correction Program*; University of Göttingen: Göttingen, Germany, 1997. (c) *XPREP*, 5.1 ed.; Siemens Industrial Automation Inc.: Madison, WI, 1995. (d) Sheldrick, G. M. *SHELXTL Reference Manual*, version 5.1; Bruker AXS: Madison, WI, 1997. (e) Sheldrick, G. M. *SHELXL-97, Program for Crystal Structure Refinement*; University of Göttingen: Göttingen, Germany, 1997.
(17) (a) Giannozzi, P.; et al. *J. Phys.: Condens. Matter* **2009**, *21*, 395502. (b) Perdew, J. P.; Burke, K.; Ernzerhof, M. *Phys. Rev. Lett.* **1996**, *77*, 3865−3868. (c) Vanderbilt, D. *Phys. Rev. B* **1990**, *41*, 7892−7895.
(18) (a) Xie, Z.; Ma, L.; deKrafft, K. E.; Jin, A.; Lin, W. *J. Am. Chem. Soc.* **2010**, *132*, 922−923. (b) Fang, Q. R.; Yuan, D. Q.; Sculley, J.; Li, J. R.; Han, Z. B.; Zhou, H. C. *Inorg. Chem.* **2010**, *49*, 11637−11642.
(19) Panda, T.; Kundu, T.; Banerjee, R. *Chem. Commun.* **2012**, *48*, 5464−5466.